Simplest and Most Predictive Model of Muon $g-2$ and Thermal Dark Matter

Ian Holst,[1,2,*] Dan Hooper,[1,2,3,†] and Gordan Krnjaic[1,2,3,‡]

[1] University of Chicago, Department of Astronomy and Astrophysics, Chicago, Illinois 60637, USA
[2] University of Chicago, Kavli Institute for Cosmological Physics, Chicago, Illinois 60637, USA
[3] Fermi National Accelerator Laboratory, Theoretical Astrophysics Group, Batavia, Illinois 60510, USA

(Received 2 August 2021; accepted 7 March 2022; published 8 April 2022)

The long-standing 4.2σ muon $g-2$ anomaly may be the result of a new particle species which could also couple to dark matter and mediate its annihilations in the early Universe. In models where both muons and dark matter carry equal charges under a $U(1)_{L_\mu - L_\tau}$ gauge symmetry, the corresponding Z' can both resolve the observed $g-2$ anomaly and yield an acceptable dark matter relic abundance, relying on annihilations which take place through the Z' resonance. Once the value of $(g-2)_\mu$ and the dark matter abundance are each fixed, there is very little remaining freedom in this model, making it highly predictive. We provide a comprehensive analysis of this scenario, identifying a viable range of dark matter masses between approximately 10 and 100 MeV, which falls entirely within the projected sensitivity of several accelerator-based experiments, including NA62, NA64μ, M^3, and DUNE. Furthermore, portions of this mass range predict contributions to $\Delta N_{\rm eff}$ which could ameliorate the tension between early and late time measurements of the Hubble constant, and which could be tested by stage 4 CMB experiments.

DOI: 10.1103/PhysRevLett.128.141802

Introduction.—Recently, the Fermilab Muon $g-2$ Collaboration presented its first measurement of the muon anomalous magnetic moment [1]. Their results are consistent with those reported by the previous Brookhaven E821 Collaboration [2], and the combined world average for $a_\mu \equiv \frac{1}{2}(g-2)_\mu$ now differs from the standard model (SM) prediction [3–23] by

$$\Delta a_\mu = (251 \pm 59) \times 10^{-11}, \tag{1}$$

constituting a 4.2σ discrepancy [24].

It is well known that MeV-scale particles which couple preferentially to muons can economically resolve the Δa_μ anomaly with muonic couplings of order $g_\mu \sim 10^{-4}$ [26–28] (for reviews of new physics explanations for the muon $g-2$ anomaly, see Refs. [29–31]). It is also well known that such particles can couple to dark matter (DM) and mediate their annihilations to SM particles, potentially leading to the production of an acceptable thermal relic abundance in the early Universe [36–42]. However, the cross section for t-channel annihilation,

$$\sigma v \sim \frac{g_\chi^4}{m_\chi^2} \sim 10^{-25}\ \mathrm{cm^3\ s^{-1}} \left(\frac{g_\chi}{10^{-2}}\right)^4 \left(\frac{\mathrm{GeV}}{m_\chi}\right)^2, \tag{2}$$

can only be sufficiently large for thermal production if $g_\chi \gg g_\mu$. A similar conclusion holds for s-channel annihilation, for which the cross section scales as $\propto g_\chi^2 g_\mu^2$, thus requiring g_χ to be even larger [40,43,44]. While scenarios with $g_\chi \gg g_\mu$ are not ruled out, this freedom reduces the predictive power of such models and imposes inelegant requirements on the gauge groups involved, posing significant challenges for their embedding in non-Abelian theories.

An exception to this lore was identified in Ref. [45], which exploits resonant annihilation in the context of a spontaneously broken $U(1)_{L_\mu - L_\tau}$ gauge group under which both the muon and the DM have comparable couplings to the corresponding gauge boson, Z'. Motivated by the latest measurement of muon $g-2$, we comprehensively analyze this scenario, identifying new parameter space that can both explain Δa_μ and yield an acceptable DM abundance for mass ratios of $m_{Z'}/m_\chi \sim 2$–3. Once the gauge coupling is fixed by the measured value of Δa_μ and the $m_\chi/m_{Z'}$ ratio is fixed by the measured DM abundance, we are left with a one-parameter family of models, making this scenario highly predictive. A combination of future laboratory measurements and cosmological observations will conclusively discover or falsify this scenario.

Model overview.—We begin by reviewing the basic features of gauged $L_\mu - L_\tau$ extensions of the SM, as introduced in Refs. [46,47]. The Lagrangian for this scenario includes

$$\mathcal{L}_{\rm int} = g' Z'_\mu (J^\mu_{\rm SM} + J^\mu_{\rm DM}), \tag{3}$$

where g' is a universal gauge coupling and Z' is the $L_\mu - L_\tau$ gauge boson. We assume that this gauge symmetry is spontaneously broken in the infrared, but that the states responsible for this breaking are sufficiently decoupled that their effects are negligible at low energies. The SM current in Eq. (3) is given by

$$J^\nu_{\rm SM} = \bar\mu\gamma^\nu\mu + \bar\nu_\mu\gamma^\nu P_L\nu_\mu - \bar\tau\gamma^\nu\tau - \bar\nu_\tau\gamma^\nu P_L\nu_\tau, \tag{4}$$

where P_L is the left chiral projector. We take the DM, χ, to be a Dirac fermion, with $J^\mu_{\rm DM} \equiv \bar\chi\gamma^\mu\chi$ (for the case of DM in the form of a complex scalar, see the Supplemental Material [48,49]).

The partial width for $Z' \to f\bar f$ decays is given by

$$\Gamma_{Z'\to f\bar f} = \frac{k_f g'^2 m_{Z'}}{12\pi}\left(1 + \frac{2m_f^2}{m_{Z'}^2}\right)\sqrt{1 - \frac{4m_f^2}{m_{Z'}^2}}, \tag{5}$$

where $k_f = 1$ for $f = \mu, \tau, \chi$ and $k_f = 1/2$ for $f = \nu_\mu, \nu_\tau$. Note that the interactions in Eq. (4) also lead to an irreducible contribution to the kinetic mixing of the Z' with the photon through μ and τ loops, of order $\varepsilon \sim g'/70$ [50]. In Fig. 1, we show the viable parameter space for this Z'.

The leading contribution to a_μ in this model arises at one loop where

$$\Delta a_\mu = \frac{g'^2}{4\pi^2}\int_0^1 dx \frac{m_\mu^2 x(1-x)^2}{m_\mu^2(1-x)^2 + m_{Z'}^2 x}, \tag{6}$$

which yields $\Delta a_\mu \approx 251 \times 10^{-11} \times (g'/4.5\times 10^{-4})^2$ in the $m_{Z'} \ll m_\mu$ limit [26]. As we will discuss below, for couplings that resolve Δa_μ, this scenario is viable for $m_{Z'} \sim 10$–200 MeV. For the remainder of this Letter, we will restrict our attention to this range of masses.

Cosmology.—To resolve the Δa_μ anomaly, the combination of Eqs. (1) and (6) implies $g' \gtrsim 10^{-4}$ for all viable values of $m_{Z'}$, as shown in Fig. 1. For couplings of this size, Z' and χ are both easily maintained in chemical equilibrium with the SM in the early Universe, so achieving the measured DM density requires an annihilation cross section of order $\sigma v \sim 5\times 10^{-26}$ cm^3 s^{-1} (for $m_\chi <$ GeV) [54].

From Eq. (2), it is clear that this cross section cannot be achieved with t-channel $\chi\bar\chi \to Z'Z'$ annihilation when the natural coupling relation is enforced, $g' = g_\mu = g_\chi$, and the DM mass is large enough to be consistent with constraints from Big Bang nucleosynthesis [55,56]. For appropriate values of $m_\chi/m_{Z'}$, however, it is possible to achieve an acceptable relic abundance through s-channel resonant annihilation.

In the very early Universe, the total number density of DM particles, $n \equiv n_\chi + n_{\bar\chi}$, is governed by the Boltzmann equation:

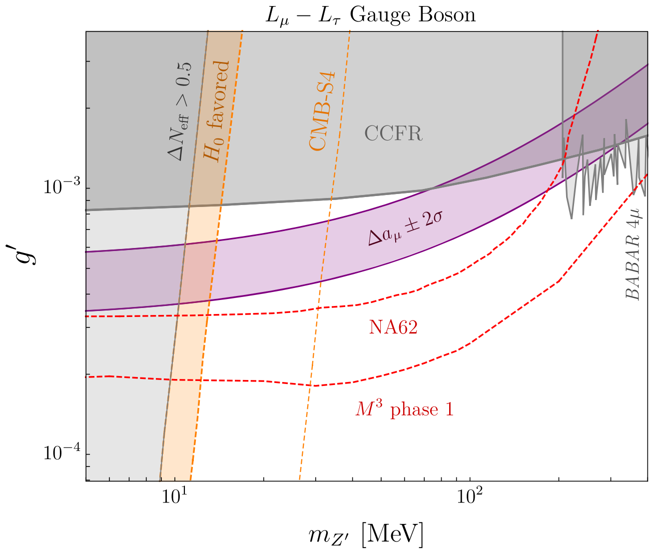

FIG. 1. The purple band represents the regions of parameter space in which an $L_\mu - L_\tau$ gauge boson can resolve the muon $g-2$ anomaly (within $\pm 2\sigma$). Inside the nearly vertical orange band, this model can also relax the H_0 tension by contributing $\Delta N_{\rm eff} \sim 0.2$–0.5 [50]; the mild slope arises from delayed neutrino decoupling via loop induced $Z' - \gamma$ kinetic mixing. The gray shaded regions represent laboratory constraints from CCFR [51,52], *BABAR* [53], and the constraint of $\Delta N_{\rm eff} > 0.5$ from measurements of the CMB and the primordial light element abundances [50]. Note that here we only show the contribution to $\Delta N_{\rm eff}$ from from the Z', without any additional contribution from dark matter annihilation. Also shown are projected sensitivity of the NA62 experiment [40], and phase 1 of the M^3 muon missing momentum experiment [43].

$$\frac{dn}{dt} + 3Hn = -\frac{1}{2}\langle\sigma v\rangle(n^2 - n_{\rm eq}^2), \tag{7}$$

where H is the Hubble rate and $n_{\rm eq}$ is the equilibrium number density. The thermally averaged annihilation cross section is [57]

$$\langle\sigma v\rangle = \frac{1}{8m_\chi^4 T K_2^2(\frac{m_\chi}{T})}\int_{4m_\chi^2}^\infty ds\sigma\sqrt{s}(s - 4m_\chi^2)K_1\left(\frac{\sqrt{s}}{T}\right), \tag{8}$$

where K_n is a modified Bessel function of the second kind. For $m_{Z'} > m_\chi$, DM annihilation proceeds mainly [58] through s-channel processes, $\chi\bar\chi \to \bar f f$, with a cross section that is given by

$$\sigma(s) = \sum_f \frac{k_f g'^4}{12\pi s}\frac{\beta_f}{\beta_\chi}\left[\frac{(s + 2m_\chi^2)(s + 2m_f^2)}{(s - m_{Z'}^2)^2 + m_{Z'}^2\Gamma_{Z'}^2}\right], \tag{9}$$

where s is the Mandelstam variable, $\beta_i = \sqrt{1 - 4m_i^2/s}$, and $\Gamma_{Z'} = \Gamma_{Z'\to\chi\bar\chi} + \sum_f \Gamma_{Z'\to f\bar f}$ with the sums over $f = \mu, \tau, \nu_{\mu,\tau}$.

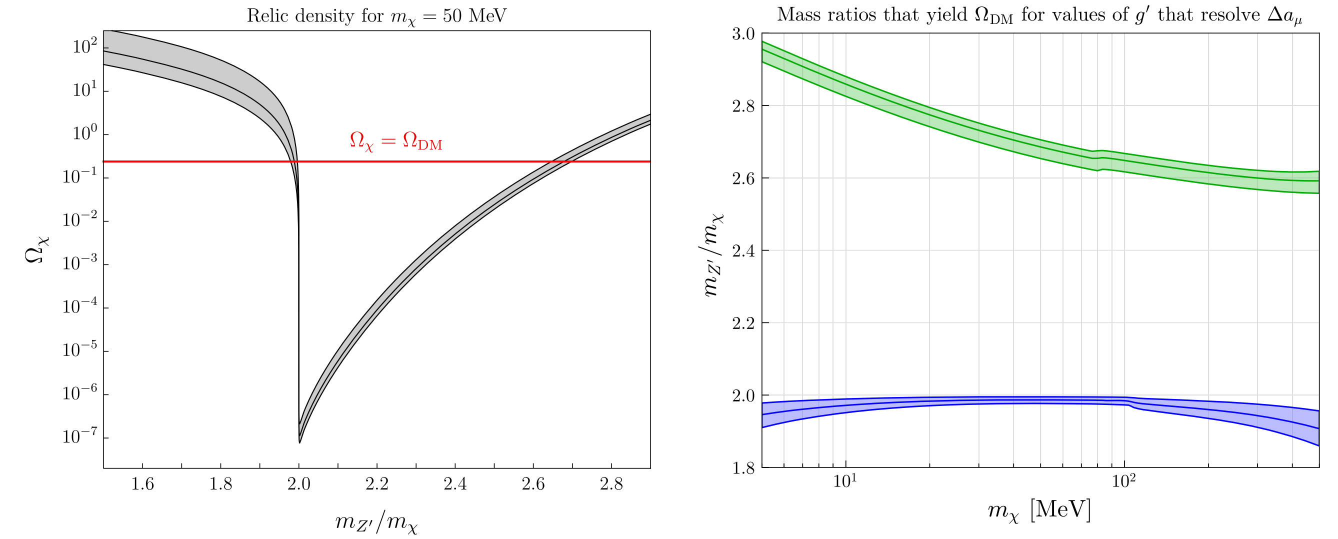

FIG. 2. Left: The dark matter relic abundance as a function of $m_{Z'}/m_\chi$, for $m_\chi = 50$ MeV, and for values of g' selected to resolve the muon $g-2$ anomaly (the thickness of the band reflects the $\pm 2\sigma$ uncertainty in the measurement of a_μ). For each choice of m_χ, there are two values of $m_{Z'}$ that can achieve the observed DM abundance indicated by the horizontal red line. Right: $m_{Z'}/m_\chi$ ratios that yield the observed DM density for the couplings that resolve Δa_μ anomaly to within $\pm 2\sigma$ at each value of $m_{Z'}$; the two bands represent the two solutions for each m_χ as shown in the left panel.

In the left panel of Fig. 2, we determine the DM relic abundance Ω_χ by numerically [61] solving Eq. (7) as a function of $m_{Z'}/m_\chi$ and fixing the coupling to obtain the measured value of $(g-2)_\mu$ for a given value of $m_{Z'}$. In the right panel we show the $m_{Z'}/m_\chi$ ratios that yield the observed density as a function of m_χ, with couplings chosen to resolve Δa_μ to within $\pm 2\sigma$. In Fig. 3, we show the regions in the $m_\chi - m_{Z'}$ plane that lead to an acceptable relic abundance, again fixing the coupling according to $(g-2)_\mu$. From these figures, we see that the measured density of DM can be obtained for either $m_{Z'}/m_\chi \approx 1.9$–$2.0$ or $m_{Z'}/m_\chi \approx 2.6$–$3.0$, which are shown in blue and green in Fig. 3, respectively. While the first band may be considered fine-tuned, we regard the other band as a prediction. Note that our results differ from the mass ratio indicated in Fig. 1 of Ref. [45].

In the mass range of interest, DM annihilations and Z' decays can each heat the SM radiation bath after the neutrinos have decoupled, thereby increasing the effective number of neutrino species,

$$\Delta N_{\rm eff} \equiv \frac{8}{7}\left(\frac{11}{4}\right)^{4/3} \frac{\delta\rho_\nu}{\rho_\gamma}\bigg|_{T=T_{\rm dec}}. \tag{10}$$

The extra energy density, $\delta\rho_\nu$, receives contributions from both $\chi\bar{\chi} \to \bar{\nu}\nu$ and $Z' \to \bar{\nu}\nu$, which take place after neutrino decoupling [69] at $T_{\rm dec} \approx 2$ MeV, leading to

$$\delta\rho_\nu \approx \int \frac{d^3\vec{p}_\chi}{(2\pi)^3} \frac{4E_\chi}{e^{E_\chi/T_{\rm dec}}+1} + \int \frac{d^3\vec{p}_{Z'}}{(2\pi)^3} \frac{3E_{Z'}}{e^{E_{Z'}/T_{\rm dec}}-1}. \tag{11}$$

Taken at face value, measurements of the CMB and baryon acoustic oscillations constrain $\Delta N_{\rm eff} \lesssim 0.3$ [67]. That being said, it has been shown that a positive value of $\Delta N_{\rm eff}$ could help to reduce the long-standing tension between local and

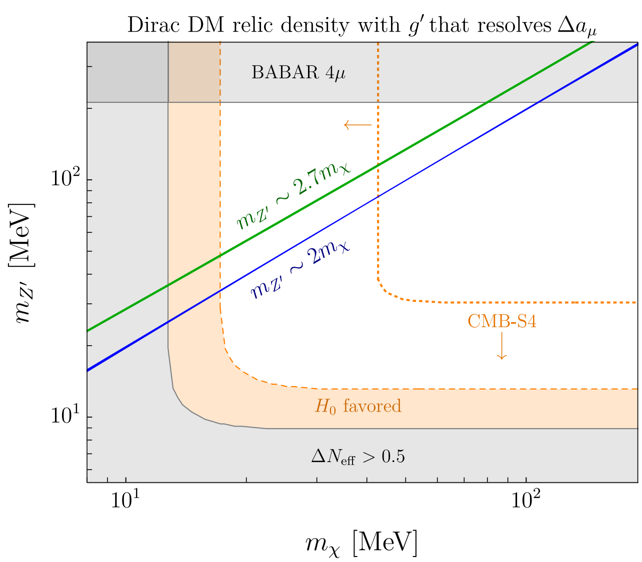

FIG. 3. In the green and blue regions, the thermal relic abundance is equal to measured density of dark matter, $\Omega_\chi h^2 \simeq 0.12$ [67], for values of g' that can resolve the muon $g-2$ anomaly to within $\pm 2\sigma$. The gray shaded regions are excluded by *BABAR* [53] and by $\Delta N_{\rm eff} > 0.5$ [50]. The orange shaded region can ameliorate the H_0 tension by contributing $0.2 < \Delta N_{\rm eff} < 0.5$, and the parameter space under and to the left of the dotted orange curve predicts $\Delta N_{\rm eff} > 0.02$, which is projected to be testable with stage 4 CMB experiments [68].

cosmological determinations of the Hubble constant, H_0 [70]. When local measurements of H_0 are included in the fit, the data prefer $\Delta N_{\mathrm{eff}} \sim 0.1$–$0.4$ [67]. With this in mind, we require that $\Delta N_{\mathrm{eff}} \lesssim 0.5$, and consider any parameter space in which $\Delta N_{\mathrm{eff}} = 0.2$–$0.5$ to be potentially capable of reducing the Hubble tension. In Fig. 3, we show isocontours of ΔN_{eff} whose shapes are computed using the approximate expression in Eq. (11) and scaled to match the more precise results given in Ref. [50,71].

Well after freeze out, the annihilation of DM particles could potentially alter the CMB's temperature anisotropies by injecting visible energy into the radiation bath during and after the era of recombination. For Dirac fermion DM, the Planck collaboration places the following constraint on such annihilations [67]:

$$p_{\mathrm{ann}} \equiv \frac{1}{2} f_{\mathrm{eff}} \frac{\langle \sigma v \rangle}{m_\chi} < 3.5 \times 10^{-28} \ \frac{\mathrm{cm}^3}{\mathrm{GeV\,s}}, \tag{12}$$

where $\langle \sigma v \rangle$ is the thermally averaged annihilation cross section at recombination, and the quantity f_{eff} parametrizes the efficiency of energy transfer to SM particles.

In our model, the only channels with non-negligible values of f_{eff} are those of $\chi\bar{\chi} \to \mu^+\mu^-$ (for which $f_{\mathrm{eff}} \sim 0.2$) and $\chi\bar{\chi} \to e^+e^-$ ($f_{\mathrm{eff}} \sim 1$) [72]. As we will discuss below, the parameter space of this model in which $m_\chi > m_\mu$ is almost entirely ruled out by laboratory constraints [73]. Because the Z' does not couple directly to electrons, $\chi\bar{\chi} \to e^+e^-$ occurs only through kinetic mixing, with a low-velocity cross section given by

$$\langle \sigma v \rangle_{\chi\bar{\chi}\to e^+e^-} \simeq \frac{(\varepsilon e g')^2 (m_e^2 + 2m_\chi^2) \sqrt{1 - m_e^2/m_\chi^2}}{2\pi[(m_{Z'}^2 - 4m_\chi^2)^2 + m_{Z'}^2 \Gamma_{Z'}^2]}. \tag{13}$$

In Fig. 4, we show the predicted value of p_{ann} for $\varepsilon = g'/70$ and values of $m_{Z'}/m_\chi$ that yield the measured density of DM. We note that while Planck's sensitivity to p_{ann} is approaching the limit of cosmic variance, future CMB experiments are expected to modestly improve upon these constraints [75].

Laboratory tests.—The Z' in this model can mediate inelastic neutrino-nucleus scattering, leading to dimuon production, $\nu_\mu N \to \nu_\mu N \mu^+\mu^-$. The CCFR experiment has measured trident production for muon neutrinos and places a limit of $m_{Z'} \lesssim 300$ MeV for couplings that can resolve the muon $g-2$ anomaly [51,52].

The properties of the Z' can also be constrained by B factories, through the $e^+e^- \to 4\mu$ channel. For couplings that resolve the muon $g-2$ anomaly, the *BABAR* experiment excludes 212 MeV $< m_{Z'} <$ 10 GeV [53]. Although our scenario includes an additional $Z' \to \chi\bar{\chi}$ decay channel throughout our mass range of interest, the phase space suppression in the parameter space of interest here renders this width negligible, allowing us to safely apply the *BABAR* limit.

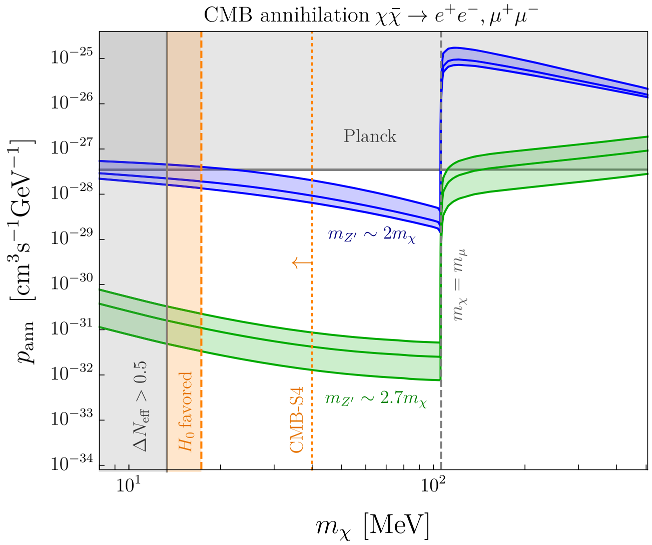

FIG. 4. Energy injection from Dirac dark matter annihilating to e^+e^- (through loop-induced kinetic mixing) and/or $\mu^+\mu^-$, during and after recombination. Following Fig. 3, the blue and green regions correspond to values of $m_{Z'}/m_\chi$, which produce the measured density of dark matter for values of g' that can resolve the muon $g-2$ anomaly to within $\pm 2\sigma$.

Since the DM does not couple directly to quarks or electrons in this model, direct detection experiments can be expected to only weakly constrain this class of scenarios. The largest contribution to the elastic scattering of DM with nuclei occurs in this model through the kinetic mixing of the Z' with the photon. For $\varepsilon = g'/70$, the cross section for DM scattering with protons is

$$\sigma_e = \frac{(\varepsilon e g')^2 m_\chi^2}{\pi m_{Z'}^4} \approx 10^{-48}\,\mathrm{cm}^2 \left(\frac{g'}{10^{-4}}\right)^4 \left(\frac{m_\chi}{100\,\mathrm{MeV}}\right)^2, \tag{14}$$

where we have used $m_\chi = 2m_{Z'}$. The cross section with electrons is further suppressed by a factor of $(m_e/m_\chi)^2 \ll 1$. Existing direct detection experiments are thus not sensitive to the scenario considered here.

Summary.—In this Letter, we have identified a simple and highly predictive model that can simultaneously resolve the muon $g-2$ anomaly and yield an acceptable dark matter relic abundance. This model introduces a leptophilic $L_\mu - L_\tau$ gauge boson whose coupling to DM and SM particles is fixed by the measured value of a_μ. Furthermore, to obtain an acceptable DM relic abundance through resonant annihilations in the early Universe, we must fix either $m_{Z'}/m_\chi \approx 1.9$–$2.0$ or $m_{Z'}/m_\chi \approx 2.6$–$3.0$. The viable range of parameter space features DM with masses in the range of $m_\chi \approx 13$–100 MeV. There is no need for *ad hoc* hierarchical charge assignments in this model, and it is naturally safe from CMB constraints.

A number of accelerator-based experiments are poised to decisively cover the relevant parameter space in this scenario. In particular, the NA62 experiment is sensitive to invisibly decaying muon-philic bosons (through $K \to \mu\nu Z'$), and may be able to cover the entire parameter space favored by the measured value of Δa_μ if systematic errors can be adequately controlled [40]. Dedicated muon beam efforts, including the CERN NA64μ [76] and Fermilab M^3 [43] experiments, are projected to cover all of the remaining parameter space for any light, invisibly decaying particles that could potentially be responsible for Δa_μ. Finally, the upcoming DUNE experiment [77,78] will improve upon existing bounds on muon trident production, covering the remaining $L_\mu - L_\tau$ parameter space that can address the muon $g-2$ anomaly. Our scenario predicts that *all* of these experiments will see a signal; a null result at any one of them would decisively falsify this model. Measurements at future fixed-target experiments could also potentially measure $m_{Z'}$ [44], allowing us (through the relic abundance) to infer the required mass of the DM candidate.

However, while laboratory searches can probe the existence of Z' and measure g' to verify this solution to Δa_μ, they cannot directly establish its possible connection to the DM of our Universe. To test this aspect of our model, it will be necessary to precisely measure both $\Delta N_{\rm eff}$ and $p_{\rm ann}$ with future CMB experiments. From Fig. 3, along the viable diagonal bands there is a one-to-one correspondence between $\Delta N_{\rm eff}$ and m_χ, so combined with a laboratory measurement of $m_{Z'}$, an observation of $\Delta N_{\rm eff}$ fixes the $m_{Z'}/m_\chi$ ratio. Since the value of g' required to resolve Δa_μ is also fixed by $m_{Z'}$, there is no additional freedom to vary the annihilation cross sections in this model. Thus, the predicted relic density from thermal freeze-out can be verified to agree with the measured value of $\Omega_{\rm DM}$ and, once the mass ratio is determined, there is a unique prediction for $p_{\rm ann}$, as shown in Fig. 4.

Data available for Fig. 2 and for the green and blue regions in Fig. 3 are available at Ref. [79].

This work is supported by the Fermi Research Alliance, LLC under Contract No. DE-AC02-07CH11359 with the U.S. Department of Energy, Office of Science, Office of High Energy Physics. I. H. received support from the Brinson Foundation.

*holst@uchicago.edu
†dhooper@fnal.gov
‡krnjaicg@fnal.gov

[1] Muon $g-2$ Collaboration, Measurement of the anomalous precession frequency of the muon in the Fermilab Muon $g-2$ Experiment, Phys. Rev. D **103**, 072002 (2021).

[2] Muon $g-2$ Collaboration, Final report of the E821 muon anomalous magnetic moment measurement at BNL, Phys. Rev. D **73**, 072003 (2006).

[3] T. Aoyama, N. Asmussen, M. Benayoun, J. Bijnens, T. Blum, M. Bruno, I. Caprini, C. Carloni Calame, M. Cè, G. Colangelo *et al.*, The anomalous magnetic moment of the muon in the Standard Model, Phys. Rep. **887**, 1 (2020).

[4] T. Aoyama, M. Hayakawa, T. Kinoshita, and M. Nio, Complete Tenth-Order QED Contribution to the Muon $g-2$, Phys. Rev. Lett. **109**, 111808 (2012).

[5] T. Aoyama, T. Kinoshita, and M. Nio, Theory of the anomalous magnetic moment of the electron, Atoms **7**, 28 (2019).

[6] A. Czarnecki, W. J. Marciano, and A. Vainshtein, Refinements in electroweak contributions to the muon anomalous magnetic moment, Phys. Rev. D **67**, 073006 (2003).

[7] C. Gnendiger, D. Stöckinger, and H. Stöckinger-Kim, The electroweak contributions to $(g-2)_\mu$ after the Higgs boson mass measurement, Phys. Rev. D **88**, 053005 (2013).

[8] M. Davier, A. Hoecker, B. Malaescu, and Z. Zhang, Reevaluation of the hadronic vacuum polarisation contributions to the Standard Model predictions of the muon $g-2$ and $\alpha(m_Z^2)$ using newest hadronic cross-section data, Eur. Phys. J. C **77**, 827 (2017).

[9] A. Keshavarzi, D. Nomura, and T. Teubner, Muon $g-2$ and $\alpha(M_Z^2)$: A new data-based analysis, Phys. Rev. D **97**, 114025 (2018).

[10] G. Colangelo, M. Hoferichter, and P. Stoffer, Two-pion contribution to hadronic vacuum polarization, J. High Energy Phys. 02 (2019) 006.

[11] M. Hoferichter, B.-L. Hoid, and B. Kubis, Three-pion contribution to hadronic vacuum polarization, J. High Energy Phys. 08 (2019) 137.

[12] M. Davier, A. Hoecker, B. Malaescu, and Z. Zhang, A new evaluation of the hadronic vacuum polarisation contributions to the muon anomalous magnetic moment and to $\alpha(m_Z^2)$, Eur. Phys. J. C **80**, 241 (2020).

[13] A. Keshavarzi, D. Nomura, and T. Teubner, The $g-2$ of charged leptons, $\alpha(M_Z^2)$ and the hyperfine splitting of muonium, Phys. Rev. D **101**, 014029 (2020).

[14] A. Kurz, T. Liu, P. Marquard, and M. Steinhauser, Hadronic contribution to the muon anomalous magnetic moment to next-to-next-to-leading order, Phys. Lett. B **734**, 144 (2014).

[15] K. Melnikov and A. Vainshtein, Hadronic light-by-light scattering contribution to the muon anomalous magnetic moment reexamined, Phys. Rev. D **70**, 113006 (2004).

[16] P. Masjuan and P. Sanchez-Puertas, Pseudoscalar-pole contribution to the $(g_\mu - 2)$: a rational approach, Phys. Rev. D **95**, 054026 (2017).

[17] G. Colangelo, M. Hoferichter, M. Procura, and P. Stoffer, Dispersion relation for hadronic light-by-light scattering: Two-pion contributions, J. High Energy Phys. 04 (2017) 161.

[18] M. Hoferichter, B.-L. Hoid, B. Kubis, S. Leupold, and S. P. Schneider, Dispersion relation for hadronic light-by-light scattering: Pion pole, J. High Energy Phys. 10 (2018) 141.

[19] A. Gérardin, H. B. Meyer, and A. Nyffeler, Lattice calculation of the pion transition form factor with $N_f = 2+1$ Wilson quarks, Phys. Rev. D **100**, 034520 (2019).

[20] J. Bijnens, N. Hermansson-Truedsson, and A. Rodríguez-Sánchez, Short-distance constraints for the HLbL contribution to the muon anomalous magnetic moment, Phys. Lett. B **798**, 134994 (2019).

[21] G. Colangelo, F. Hagelstein, M. Hoferichter, L. Laub, and P. Stoffer, Longitudinal short-distance constraints for the hadronic light-by-light contribution to $(g-2)_\mu$ with large-N_c Regge models, J. High Energy Phys. 03 (2020) 101.

[22] T. Blum, N. Christ, M. Hayakawa, T. Izubuchi, L. Jin, C. Jung, and C. Lehner, Hadronic Light-by-Light Scattering Contribution to the Muon Anomalous Magnetic Moment from Lattice QCD, Phys. Rev. Lett. **124**, 132002 (2020).

[23] G. Colangelo, M. Hoferichter, A. Nyffeler, M. Passera, and P. Stoffer, Remarks on higher-order hadronic corrections to the muon $g-2$, Phys. Lett. B **735**, 90 (2014).

[24] Although a recent lattice calculation of the SM prediction for a_μ by the BMW Collaboration [25] is closer to the measured value, it is also in tension with the consensus SM prediction, driven by R-ratio calculations [3]. Future lattice calculations and improved R-ratio data will likely be needed to clarify this situation.

[25] S. Borsanyi, Z. Fodor, J. N. Guenther, C. Hoelbling, S. D. Katz, L. Lellouch, T. Lippert, K. Miura, L. Parato, K. K. Szabo *et al.*, Leading hadronic contribution to the muon magnetic moment from lattice QCD, Nature (London) **593**, 51 (2021).

[26] M. Pospelov, Secluded U(1) below the weak scale, Phys. Rev. D **80**, 095002 (2009).

[27] C.-Y. Chen, M. Pospelov, and Y.-M. Zhong, Muon beam experiments to probe the dark sector, Phys. Rev. D **95**, 115005 (2017).

[28] P. Fayet, U-boson production in e^+e^- annihilations, ψ and Υ decays, and light dark matter, Phys. Rev. D **75**, 115017 (2007).

[29] P. Athron, C. Balázs, D. H. J. Jacob, W. Kotlarski, D. Stöckinger, and H. Stöckinger-Kim, New physics explanations of a_μ in light of the FNAL muon $g-2$ measurement, J. High Energy Phys. 09 (2021) 080.

[30] R. Capdevilla, D. Curtin, Y. Kahn, and G. Krnjaic, A no-lose theorem for discovering the new physics of $(g-2)_\mu$ at muon colliders, Phys. Rev. D **105**, 015028 (2022).

[31] Dark photons and similar $U(1)$ extensions (e.g., gauged $B-L$) featuring appreciable couplings to first generation fermions have been excluded as explanations for Δa_μ [32,33]. Similar conclusions hold for light Higgs-mixed scalars and for leptophilic scalars with couplings proportional to their mass [34,35].

[32] M. Bauer, P. Foldenauer, and J. Jaeckel, Hunting all the hidden photons, J. High Energy Phys. 07 (2018) 094.

[33] P. Ilten, Y. Soreq, M. Williams, and W. Xue, Serendipity in dark photon searches, J. High Energy Phys. 06 (2018) 004.

[34] G. Krnjaic, Probing light thermal dark matter with a Higgs portal mediator, Phys. Rev. D **94**, 073009 (2016).

[35] *BABAR* Collaboration, Search for a Dark Leptophilic Scalar in e^+e^- Collisions, Phys. Rev. Lett. **125**, 181801 (2020).

[36] A. Kamada, K. Kaneta, K. Yanagi, and H.-B. Yu, Self-interacting dark matter and muon $g-2$ in a gauged $\mathrm{U}(1)_{L_\mu - L_\tau}$ model, J. High Energy Phys. 06 (2018) 117.

[37] S. Singirala, S. Sahoo, and R. Mohanta, Light dark matter, rare B decays with missing energy in $L_\mu - L_\tau$ model with a scalar leptoquark, Phys. Rev. D **105**, 015033 (2022).

[38] D. Borah, M. Dutta, S. Mahapatra, and N. Sahu, Muon $(g-2)$ and XENON1T excess with boosted dark matter in $L_\mu - L_\tau$ model, Phys. Lett. B **820**, 136577 (2021).

[39] A. Biswas and A. Shaw, Reconciling dark matter, $R_{K^{(*)}}$ anomalies and $(g-2)_\mu$ in an $L_\mu - L_\tau$ scenario, J. High Energy Phys. 05 (2019) 165.

[40] G. Krnjaic, G. Marques-Tavares, D. Redigolo, and K. Tobioka, Probing Muonphilic Force Carriers and Dark Matter at Kaon Factories, Phys. Rev. Lett. **124**, 041802 (2020).

[41] M. Drees, M. Shi, and Z. Zhang, Constraints on $U(1)_{L_\mu - L_\tau}$ from LHC Data, Phys. Lett. B **791**, 130 (2019).

[42] N. Okada and O. Seto, Inelastic extra $U(1)$ charged scalar dark matter, Phys. Rev. D **101**, 023522 (2020).

[43] Y. Kahn, G. Krnjaic, N. Tran, and A. Whitbeck, M^3: A new muon missing momentum experiment to probe $(\mathrm{g}-2)_\mu$ and dark matter at Fermilab, J. High Energy Phys. 09 (2018) 153.

[44] N. Blinov, G. Krnjaic, and D. Tuckler, Characterizing dark matter signals with missing momentum experiments, Phys. Rev. D **103**, 035030 (2021).

[45] P. Foldenauer, Light dark matter in a gauged $U(1)_{L_\mu - L_\tau}$ model, Phys. Rev. D **99**, 035007 (2019).

[46] X.-G. He, G. C. Joshi, H. Lew, and R. R. Volkas, New-Z' phenomenology, Phys. Rev. D **43**, R22 (1991).

[47] X.-G. He, G. C. Joshi, H. Lew, and R. R. Volkas, Simplest Z' model, Phys. Rev. D **44**, 2118 (1991).

[48] See Supplemental Material at http://link.aps.org/supplemental/10.1103/PhysRevLett.128.141802 for the case of scalar dark matter and additional detail on post-freeze out annihilation near resonance.

[49] Throughout this study, we will assume that the DM carries one unit of $L_\mu - L_\tau$ charge. If another charge assignment is selected, the effective coupling of the Z' to the DM will be shifted by this quantity.

[50] M. Escudero, D. Hooper, G. Krnjaic, and M. Pierre, Cosmology with a very light $L_\mu - L_\tau$ gauge boson, J. High Energy Phys. 03 (2019) 071.

[51] S. R. Mishra, S. A. Rabinowitz, C. Arroyo, K. T. Bachmann, R. E. Blair, C. Foudas, B. J. King, W. C. Lefmann, W. C. Leung, E. Oltman *et al.*, Neutrino Tridents and W—Z Interference, Phys. Rev. Lett. **66**, 3117 (1991).

[52] W. Altmannshofer, S. Gori, M. Pospelov, and I. Yavin, Neutrino Trident Production: A Powerful Probe of New Physics with Neutrino Beams, Phys. Rev. Lett. **113**, 091801 (2014).

[53] *BABAR* Collaboration, Search for a muonic dark force at *BABAR*, Phys. Rev. D **94**, 011102 (2016).

[54] G. Steigman, B. Dasgupta, and J. F. Beacom, Precise relic WIMP abundance and its impact on searches for dark matter annihilation, Phys. Rev. D **86**, 023506 (2012).

[55] C. Bœhm, M. J. Dolan, and C. McCabe, A lower bound on the mass of cold thermal dark matter from Planck, J. Cosmol. Astropart. Phys. 08 (2013) 041.

[56] K. M. Nollett and G. Steigman, BBN and the CMB constrain neutrino coupled light WIMPs, Phys. Rev. D **91**, 083505 (2015).

[57] P. Gondolo and G. Gelmini, Cosmic abundances of stable particles: Improved analysis, Nucl. Phys. **B360**, 145 (1991).

[58] While annihilations through the "forbidden" channel, $\chi\bar{\chi} \to Z'Z'$, may also be possible [59,60], this is subdominant in the parameter space close to the resonance region.

[59] K. Griest and D. Seckel, Three exceptions in the calculation of relic abundances, Phys. Rev. D **43**, 3191 (1991).

[60] R. T. D'Agnolo and J. T. Ruderman, Light Dark Matter from Forbidden Channels, Phys. Rev. Lett. **115**, 061301 (2015).

[61] Our numerical results were obtained using FeynCalc [62–64] and Astropy [65,66].

[62] R. Mertig, M. Böhm, and A. Denner, FeynCalc—Computer-algebraic calculation of Feynman amplitudes, Comput. Phys. Commun. **64**, 345 (1991).

[63] V. Shtabovenko, R. Mertig, and F. Orellana, New developments in FeynCalc9.0, Comput. Phys. Commun. **207**, 432 (2016).

[64] V. Shtabovenko, R. Mertig, and F. Orellana, FeynCalc 9.3: New features and improvements, Comput. Phys. Commun. **256**, 107478 (2020).

[65] Astropy Collaboration, Astropy: A community PYTHON package for astronomy, Astron. Astrophys. **558**, A33 (2013).

[66] Astropy Collaboration, The astropy project: Building an open-science project and status of the v2.0 core package, Astron. J. **156**, 123 (2018).

[67] Planck Collaboration, Planck 2018 results: VI. Cosmological parameters, Astron. Astrophys. **641**, A6 (2020).

[68] CMB-S4 Collaboration, *CMB-S4 Science Book*, 1st ed. (2016), arXiv:1610.02743.

[69] Note that χ and Z' entropy transfers that contribute to ΔN_{eff} occur while the DM is still in chemical equilibrium and freeze out occurs below T_{dec}, though the DM number density is already Boltzmann suppressed at T_{dec}. Thus, by energy conservation, the total energy density in Eq. (11) must be transferred to neutrinos; since the DM is particle or antiparticle symmetric and in equilibrium at T_{dec}, there is no chemical potential in Eq. (11).

[70] E. Di Valentino, O. Mena, S. Pan, L. Visinelli, W. Yang, A. Melchiorri, D. F. Mota, A. G. Riess, and J. Silk, In the realm of the Hubble tension-a review of solutions, Classical Quantum Gravity **38**, 153001 (2021).

[71] In the $m_\chi \gg m_{Z'}$ limit, only Z' contributes to N_{eff}, matching the scenario explored in Ref. [50]. In the opposite limit, only χ contributes, so N_{eff} can be extracted by rescaling the spin degrees-of-freedom between χ and Z' in the limit of Maxwell-Boltzmann statistics.

[72] T. R. Slatyer, Indirect dark matter signatures in the cosmic dark ages. I. Generalizing the bound on s-wave dark matter annihilation from Planck results, Phys. Rev. D **93**, 023527 (2016).

[73] While there are limits on DM annihilation to muons in similar models from the AMS-02 experiment [74], that annihilation channel is already excluded in our model. AMS-02 is also not sensitive to the range of m_χ that we consider.

[74] L. Zu, X. Pan, L. Feng, Q. Yuan, and Y.-Z. Fan, Constraining $U(1)_{L_\mu - L_\tau}$ charged dark matter model for muon $g-2$ anomaly with AMS-02 electron and positron data, arXiv:2104.03340.

[75] D. Green, P. D. Meerburg, and J. Meyers, Aspects of dark matter annihilation in cosmology, J. Cosmol. Astropart. Phys. 04 (2019) 025.

[76] S. N. Gninenko, N. V. Krasnikov, and V. A. Matveev, Search for dark sector physics with NA64, Phys. Part. Nucl. **51**, 829 (2020).

[77] DUNE Collaboration, Volume I. Introduction to DUNE, J. Instrum. **15**, T08008 (2020).

[78] P. Ballett, M. Hostert, S. Pascoli, Y. F. Perez-Gonzalez, Z. Tabrizi, and R. Z. Funchal, Z's in neutrino scattering at DUNE, Phys. Rev. D **100**, 055012 (2019).

[79] I. Holst, D. Hooper, and G. Krnjaic, Dark matter and Z' masses preferred by muon $g-2$ and thermal freeze-out, (2021) 10.5281/zenodo.5153939.